Research Article | Vol. 13, No. 5 / 1 May 2023 / Optical Materials Express 1372
Optical Materials EXPRESS

3D printing of colored micro-optics

VALESE ASLANI,[1,2,*] ANDREA TOULOUSE,[1,2] MICHAEL SCHMID,[2,3] HARALD GIESSEN,[2,3] TOBIAS HAIST,[1,2] AND ALOIS HERKOMMER[1,2]

[1]Institute of Applied Optics, University of Stuttgart, Pfaffenwaldring 9, 70569 Stuttgart, Germany
[2]Research Center SCoPE, University of Stuttgart, Pfaffenwaldring 57, 70569 Stuttgart, Germany
[3]4th Physics Institute, University of Stuttgart, Pfaffenwaldring 57, 70569 Stuttgart, Germany
[*]aslani@ito.uni-stuttgart.de

Abstract: Commercially available optical photoresists for femtosecond direct laser writing are mostly transparent and only cover a small range of optical properties. This limits the design possibilities of micro-structures and micro-optics. Although the fabrication of 3D-printed micro-optics has become state of the art, the field of spectral filtering seems to be widely unexplored. In this work, we present, evaluate and compare different methods that can be used to fabricate colored micro-elements based on the already available polymers by adding pigments or dyes to the photoresists or by dyeing the fabricated structures in a post-printing process. Both optical performance and spectral filtering results are promising and could enable integrated color filtering or hyperspectral imaging in the field of 3D-printed micro-optics.

1. Introduction

In recent years the fabrication of 3D-printed micro-optics and other 3D-printed micro-structures has become state of the art [1–12]. There are many different applications for which 3D-printed structures can be used, for example micro-optical systems [13–18], endoscopy [19,20], biology [21–23], microfluidics [24,25] or spectroscopic measurements [26]. Also luminescent 3D structures [27], graded plasmonic devices [28] and quantum dot light-emitting diodes [29] were previously fabricated. Nevertheless, one is mostly dependent on the photoresists that are available for printing, which limits the design possibilities of optical systems. Most commercially available resists can only be used to produce primarily transparent printed optical surfaces, apertures and support structures. Therefore, stray light can cause an undesired contrast loss. Intransparent apertures are thus crucial and several methods were developed to overcome this constraint by filling integrated 3D-printed cavities with black ink [30], shadow evaporation [31], or using a novel highly absorptive photoresist, which can be polymerized via femtosecond direct laser writing (fs DLW) [32].

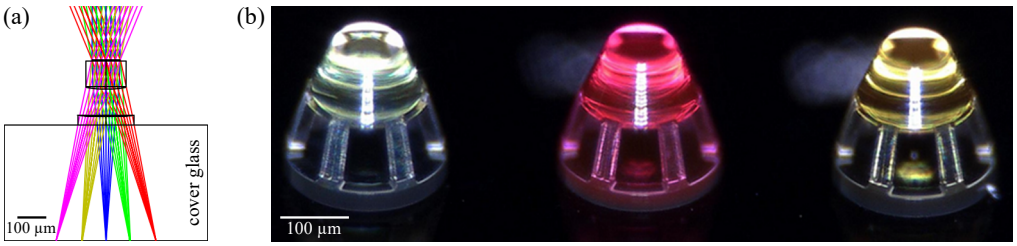

Fig. 1. Colored micro-optics. (a) Optical design of the lens system. (b) Microscope image of multiple micro-optics of different color printed successively on the same glass substrate.

#489681 https://doi.org/10.1364/OME.489681
Journal © 2023 Received 16 Mar 2023; revised 15 Apr 2023; accepted 17 Apr 2023; published 25 Apr 2023

Optical Materials EXPRESS

One possibility to expand the application area for 3D-printed micro-structures and micro-optics is the fabrication of colored structures (Fig. 1) that filter out only a specific range of the spectrum, since the field of spectral filtering by photoresists seems to be widely unexplored. Due to the fact that the available transparent resists show good results for the fs DLW process, we focus on methods using those resists as basic media. Here the fabricated micro-structures are dyed by adding other substances to the resists before printing or coloring them in a post-printing process.

The use of spectral filtering can lead to improved optical performance by reducing chromatic aberrations, but might also serve to introduce additional information channels, e.g. for spectral identification. Especially in the area of medical technologies hyperspectral imaging shows great potential for non-invasive disease diagnosis [33], enables early detection of malignant lesions and helps at cancer diagnosis [34]. The availability of tailored colored micro-optics could be a key factor to drive current methods towards miniaturization and non-invasiveness.

In endoscopy, commercially available systems, which enhance the color contrast through the change of the effective spectral response, are already in use [35,36]. White Light Imaging (WLI) uses white light with a large wavelength range to illuminate the tissue while in Narrow Band Imaging (NBI) the tissue is just illuminated with light of selected wavelengths. When illuminating a specimen, light of certain wavelengths is absorbed and certain wavelengths are reflected due to the properties of the object. One can take advantage of this by filtering out all wavelengths of the illumination spectrum except the ones of the absorption spectrum of hemoglobin. The hemoglobin in the blood vessels absorbs these specific wavelengths while they are reflected by the surrounding tissue, which enhances the contrast between these structures. Since tumorous tissue is often surrounded by a higher number of blood vessels, this criteria can be used to differentiate between healthy tissue and pathologically changed tissue. Because of the better contrast that can be achieved by the usage of the NBI technology, a better and sometimes earlier identification of tumors can be achieved [37–39]. In combination with 3D-printed micro-optical elements such techniques could be miniaturized further to expand the diagnostic options.

With the aim of producing colored micro-structures and micro-optics, we developed several manufacturing processes based on fs DLW and the commercial photoresist IP-S. In this work, three methods for dyeing micro-elements are presented. For the first the manufactured structures were colored after printing, for the second method a color pigment was added to the liquid photoresist before printing. For the third method a colored liquid resist based on an organic dye was added to the commercial photoresist before the polymerization process. An imaging system was designed and manufactured in order to evaluate the developed manufacturing processes and test their suitability for the fabrication of micro-optical systems with optical surface quality. Furthermore, plates of different heights, which can be used as spectral filters, were fabricated. UV-cured samples of the colored resists were used for refractive index measurements. Several laboratory setups were used to evaluate the imaging performance of the micro-lenses, to measure the refractive index of the colored resists, and to analyse their transmission spectra.

2. Materials and methods

The micro-optical system was designed and optimized using the sequential mode of the optical design software ZEMAX. The two-lens system is rotationally symmetric, has a field of view of 45°, a diameter of 193.5 µm, a height of 224.6 µm, a focal length of 400 µm, an f-number of 4.3, and the sequential surface-type even asphere was used for the surfaces in order to eliminate aberrations. The optical design is shown in Fig. 1(a). The theoretical modulation transfer function (MTF) of the designed optical system is shown in Fig. S1 of the supplemental document. The optical system was designed such that the second lens is directly attached to the substrate on which the micro-optics are printed on and that the image plane is on the back side of the glass substrate (Haemacytometer Cover Slips, 24 x 24 mm, thickness: 0.4 mm, Gerhard Menzel GmbH, Braunschweig, Germany). It was designed this way so that the optical system can easily

Optical Materials EXPRESS

be adapted to be used and printed on the cover glass of an image sensor. The optimized optical system was converted into a stereolithographic file format and exported to the computer-aided design software SolidWorks, where a lens mount was added. The overall system with the mount has a diameter of 233.5 µm and a height of 224.6 µm.

All micro-elements presented in this work were fabricated by dip-in fs DLW using the Photonic Professional GT2 (Nanoscribe GmbH, Karlsruhe, Germany) with a pulsed femtosecond fiber laser at a center wavelength of 780 nm and a 25x objective (LCI Plan-Neofluar 25x/NA0.8, Carl Zeiss Microscopy Deutschland GmbH, Germany). In the case of printing with colored resists the objective was protected with a thin cling foil as described in [40], using the wrapped writing configuration. This enables printing in dip-in mode without any contact of the colored resist with the objective and avoids damage and discoloration of the objective. As immersion medium Zeiss Immersol 518 F was used. After printing all presented micro-optics and micro-structures were put into a propylene glycol methyl ether acetate (mr-Dev 600, Micro Resist Technology, Berlin, Germany) bath for twelve minutes to remove residual photoresist and were rinsed in an isopropanol bath for two minutes afterwards.

There are several ways to realize color filtering in 3D-printed optical imaging systems. One possibility is to first fabricate a filter plate with the colored resist and then print a transparent micro-lens right above the filter plate for optical imaging. Another possibility is to directly print the micro-optics using a colored resist or to dye the micro-optics after printing. In the following we will present and compare the results we achieved by using the three techniques mentioned in the beginning for the manufacturing of colored micro-optics and spectral filter plates.

For dyeing method 1, we dyed a micro-lens fabricated from IP-S by conventional fs DLW after printing. Similar to [41] a dye solution was prepared comprising 50 ml acetone and 50 mg Eosin Y (C.I. 45380), which should dye the lens red. The solution and a stir bar were added into a beaker, sealed it with parafilm and stirred for 30 minutes with a magnetic stirrer. After that, the solution was left to stand for 24 hours so that undissolved dye could settle at the bottom of the beaker. The solution was transferred into another beaker so that the undissolved residues remain behind. After 3D printing and development, the substrate with the micro-optic was laid in a container, which was filled up with the dye solution and in which the substrate was left for 24 hours. In a next step the substrate was removed from the container and washed with distilled water.

For dyeing method 2, a printable colored photoresist was manufactured by adding a color pigment (Eosin Y, C.I. 45380) to the commercial photoresist IP-S. The solution was mixed with a magnetic stirrer and used to print the presented micro-optical system.

For dyeing method 3, a colored resist based on an organic dye (SX AR-N, Allresist GmbH, Strausberg, Germany) [42] was added to the photoresist before printing. In this case we used the red SX AR-N since we also dyed the other lenses red by using Eosin Y. A small amount of red SX AR-N was added to the IP-S (mixing ratio 1:10) and mixed with a magnetic stirrer. This solution was used for printing.

The fabricated structures and their imaging performance were observed using a commercial digital microscope (VHX-7000 digital microscope, VH-Z50L long-focal-distance, high-performance zoom lens (50x to 500x), KEYENCE CORPORATION, Osaka, Japan) and white light for illumination. Pictures of the imaging performance of the micro-lenses were taken by focusing on the image plane located on the backside of the glass substrate the micro-optics were printed on.

A 1951 USAF resolution test chart (2"x2" Negative, USAF 1951 Hi-Resolution Target, Edmund Optics, Barrington, USA) was used as optical resolution test device to evaluate the imaging performance of the printed micro-optics. The target was placed at a distance of 10 mm behind the micro-lens and illuminated from the back, using white light for transmitted light illumination.

To examine the optical properties of the commonly used IP-S and the resists used for dyeing method 3, we performed refractive index measurements for the resists. The samples were

Optical Materials EXPRESS

illuminated with a UV light-curing spot lamp system (BlueWave 50, Dymax Europe GmbH, Wiesbaden, Germany) delivering 365 nm with an intensity of 3000 mW/cm^2, at a distance of 3 cm with resulting intensity of 250 mW/cm^2, for 30 minutes and additionally post baked at 80 °C for one hour. The refractive index measurements where performed using a multi-wavelength dispersion refractometer (ATR L, SCHMIDT + HAENSCH GmbH & Co., Berlin, Germany) measuring the dispersion in the visible at seven wavelengths (400 nm, 486 nm, 587 nm, 656 nm, 706 nm, 780 nm and 900 nm).

Furthermore, the transmission spectra of the micro-elements fabricated using method 3 were examined using a commercial spectrometer (Avantes, AvaSpec-ULS2048CL-EVO, Apeldoorn, Netherlands). For illumination a stabilized fiber-coupled Tungsten-Halogen Light Source (SLS201L/M, wavelength range 360-2600 nm, Thorlabs, Newton, United States) was used, whose output facet was imaged onto the relevant structures with a 50x microscope objective (M Plan APO, 50x/NA0.55, Edmund Optics, Barrington, USA). In order to gain spectral information, the light that is transmitted through the specimen is collected with an 20x microscope objective (M Plan APO, 20x/NA0.42, Edmund Optics, Barrington, USA), directed to the spectrometer and thus recorded.

3. Results and discussion

3.1. Dyeing methods

The results of the tested methods are summarized in Fig. 2. Since all demonstrated micro-structures are based on the photoresist IP-S, we first printed the mentioned micro-lens using pure IP-S (Fig. 2(a)) without any additions. The colored lens systems (Fig. 2(b)-(d)) are compared to the IP-S lens in terms of image quality and their behavior during printing. We used a digital microscope to take pictures of all micro-optics, their bottom lens and of their image plane. To evaluate the imaging performance of the lens systems, a 1951 USAF resolution test chart was observed with the micro-lenses.

In Fig. 2(a) a conventionally printed IP-S lens is shown for comparison. The picture taken during the printing process shows that no noticeable irregularities occurred during this standard printing process. The performance test with the USAF chart shows a resolution up to the last element of the third group, where the linewidth corresponds to about 35 µm in the object plane.

Figure 2(b) shows the micro-lens, which was dyed after printing a IP-S lens like shown in Fig. 2(a) using dyeing method 1. The coloring process works since the lens system was successfully dyed red, but it seems like the acetone affects the surfaces and the shape accuracy of the fabricated structure, which can also be seen in the changes in the image of the bottom lens. Furthermore, it can be noticed that particles have deposited around and probably also on the lens. Presumably due to the change of shape and the deposited particles it was not possible to get a useful image at the image plane. Yet the process can still be useful for dyeing micro-structures for which the surface accuracy does not particularly matter. The structures can be printed as usual, which could be beneficial in some cases and the color can be adjusted after printing. Nevertheless, the post-printing dyeing takes some extra time.

In Fig. 2(c) the lens system printed by using dyeing method 2, which adds dye to the liquid photoresist before polymerization, is shown. Again, a dyed micro-structure could successfully be fabricated, but bubbles occurred during the printing process, which can also be seen in the image of the bottom lens of the cured and developed lens system. Since this did not happen for the lens printed with pure IP-S, the reason for this could be the interaction of the laser with the added color pigments during the fs DLW process. We were still able to get an optical image, but the imaging performance was deteriorated by the bubbles and the resulting surface deformations in the lens system in comparison to the lens shown in Fig. 2(a). Also the image contrast is weak and we only got a pale red coloration for this method. A greater amount of pigments could be added

Optical Materials EXPRESS

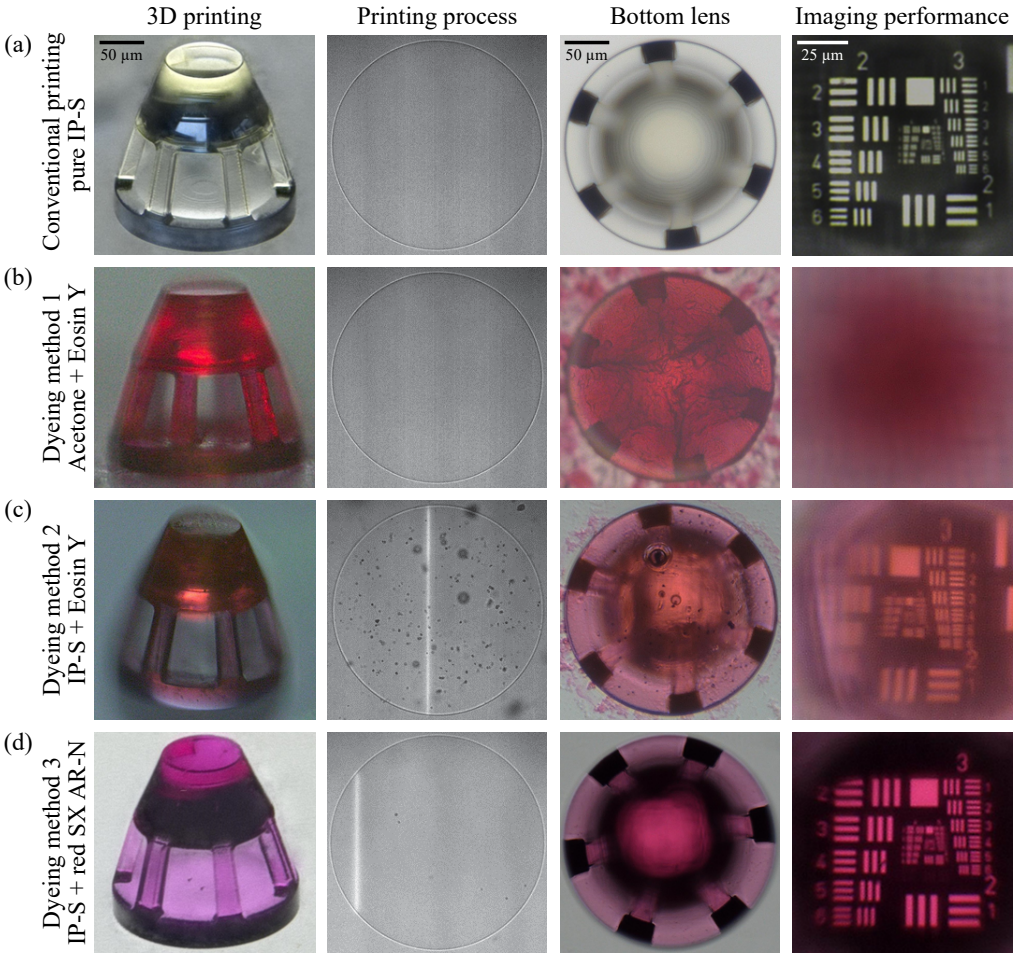

Fig. 2. Comparison of the different methods for dyeing 3D-printed micro-structures. (a) Conventionally printed micro-lens fabricated using pure IP-S. (b) Dyeing method 1: Micro-lens dyed in a post-printing process using a solution of acetone and Eosin Y. (c) Dyeing method 2: Micro-lens printed using a mixture of IP-S and Eosin Y. (d) Dyeing method 3: Micro-lens printed using a mixture of IP-S and red SX AR-N. The images show from left to right the 3D-printed micro-optics, pictures taken during the fs DLW printing process, images of the bottom lenses, and the imaging performance of the lens systems. A more detailed evaluation of the imaging performance of the IP-S lens (a) and the red SX AR-N lens (d) is presented in Fig. 3.

to the IP-S to perhaps get a more saturated color, but the larger amount of pigments will most likely lead to the occurrence of even more bubbles.

For the lens system printed using dyeing method 3, where SX AR-N is added to the IP-S, no bubbles could be observed while printing as shown in Fig. 2(d). With this method the micro-lens could clearly be colored red as shown in the left image and also the filtering effect is visible in the right image of Fig. 2(d). At first sight, the imaging performance did not significantly degrade compared to the IP-S lens. The imaging performance will be investigated further in Fig. 3. We also performed surface roughness and surface deviation measurements and found no significant degradation for the SX AR-N lens in comparison to the IP-S lens. The measurements were added to the supplemental document.

Optical Materials EXPRESS

In summary, method 3 outperformed methods 1 and 2 in handling, surface and imaging quality. Therefore, we focus on colored micro-optics fabricated using method 3 in our further analyses.

3.2. Imaging performance

In order to be able to evaluate the imaging performance of the SX AR-N micro-lens better, we compared the RGB-profiles of an intensity cut through the third group of the image of the USAF chart for the IP-S lens (conventional printing, lens shown in 2(a)) and the SX AR-N lens (fabricated by using dying method 3, lens shown in 2(d)). The results are shown in Fig. 3. For the IP-S lens the three bars of the sixth element of the third group can be perceived separately from each other and that the RGB-profiles all approximately have the same intensity. For the red SX AR-N lens, there is a slight performance loss since the fifth element of the third group is the last element that can be resolved with this lens. Nevertheless, the filtering effect of the red lens becomes clear, since lower intensity values can be observed for the green and blue profiles in comparison to the intensity distribution of the dominant red profile. The reasons for the performance loss could be process-dependent variations of the fs DLW process or based on possible changes of the optical properties of the mixtures due to the dye that was added to the IP-S.

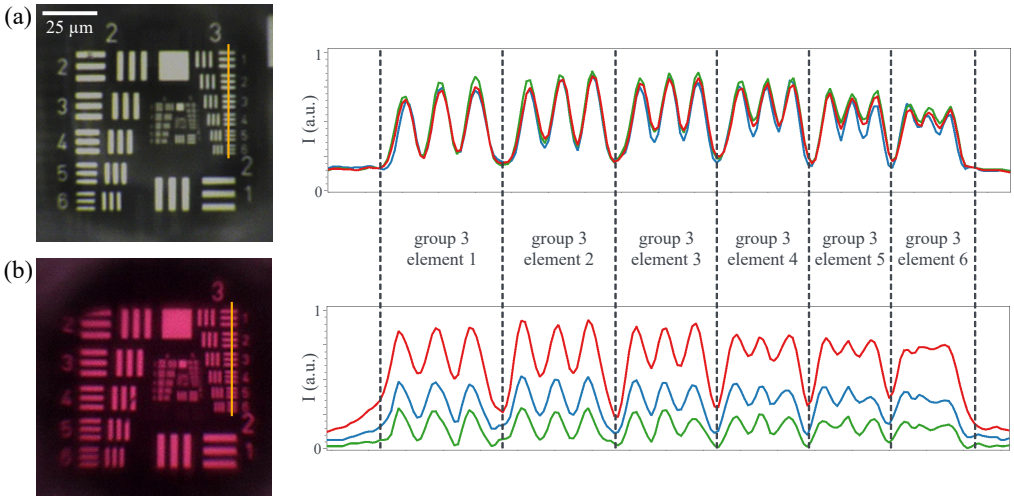

Fig. 3. Image of the USAF resolution chart for (a) IP-S lens and (b) red SX AR-N lens dyed using method 3 and their RGB intensity profiles, respectively, through a cut along the orange lines.

3.3. Refractive index measurement

Especially for optical imaging systems the refractive index of the material has to be considered in the design, which makes the knowledge about the dispersion crucial. Refractive index measurements for different common photoresists used for fs DLW were already presented in [43]. To examine the optical properties of our resists, the refractive index profile was measured for IP-S only and for a mixture of IP-S with the four available SX AR-N colors red, yellow, green and blue (mixing ratio 10:1), respectively. The samples were illuminated with a UV lamp for 30 minutes, post baked at 80 °C for one hour and the refractive index measurements where performed using a multi-wavelength dispersion refractometer. The results are shown in Fig. 4, where the dots mark the measured data points and the dashed lines represent the Cauchy fits, calculated using the fit

Optical Materials EXPRESS

function

$$n(\lambda) = A + \frac{B}{\lambda^2} + \frac{C}{\lambda^4}. \quad (1)$$

The fit parameters are summarized in Table 1. It can be seen that in comparison to the measurement of the pure IP-S, the refractive index for the mixtures of IP-S and SX AR-N are slightly higher. The discontinuities visible in the plot are probably due to absorption in the visible. For the green resist this is also indicated by the measurement of the transmission spectra in Fig. 8, where the filter plates show high absorbance in the wavelength range from 570 nm to 680 nm. In the future, the results of this measurement can already be taken into account in the optical design to improve the performance of the printed micro-optics.

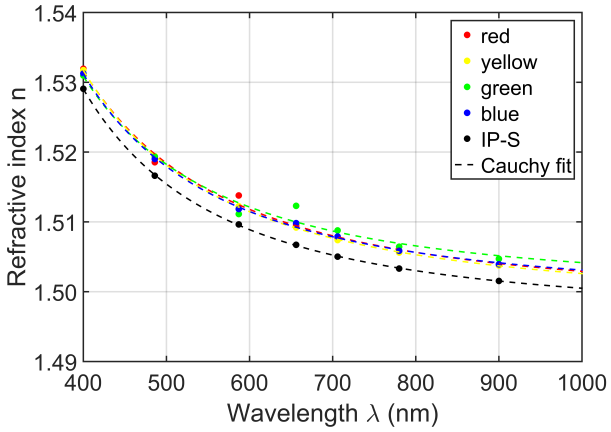

Fig. 4. Refractive index measurement for the photoresist IP-S and for mixtures of IP-S with the four available SX AR-N colors of dying method 3 red, yellow, green and blue in the visible. The samples were illuminated with a UV lamp for 30 minutes, post baked at 80°C for one hour and the measurements were performed using a multi-wavelength dispersion refractometer (ATR L, SCHMIDT + HAENSCH GmbH & Co., Berlin, Germany).

Table 1. Cauchy parameters for IP-S and for mixtures of IP-S with the four available SX AR-N colors of dying method 3 red, yellow, green and blue, respectively. The parameters were used to calculate the Cauchy fits that are presented in Fig. 4 using Eq. (1).

	A	B	C
IP-S	1.4964	$3.9355 \cdot 10^{-3}$	$2.0702 \cdot 10^{-4}$
IP-S + SX AR-N red	1.4983	$4.4556 \cdot 10^{-3}$	$1.4066 \cdot 10^{-4}$
IP-S + SX AR-N yellow	1.4981	$4.3791 \cdot 10^{-3}$	$1.6118 \cdot 10^{-4}$
IP-S + SX AR-N green	1.5002	$3.8172 \cdot 10^{-3}$	$1.7504 \cdot 10^{-4}$
IP-S + SX AR-N blue	1.4989	$4.0315 \cdot 10^{-3}$	$1.8197 \cdot 10^{-4}$

3.4. Long-term stability

To ensure that long-term stability is given for the micro-optics printed using dyeing method 3 and that there is no significant degradation in performance (for example due to solvent evaporation), we took pictures of the micro-lens and its imaging performance with a digital microscope directly after printing and three months after the printed structures were stored under room conditions. Figure 5 shows that there is no significant difference in the performance between the

Optical Materials EXPRESS

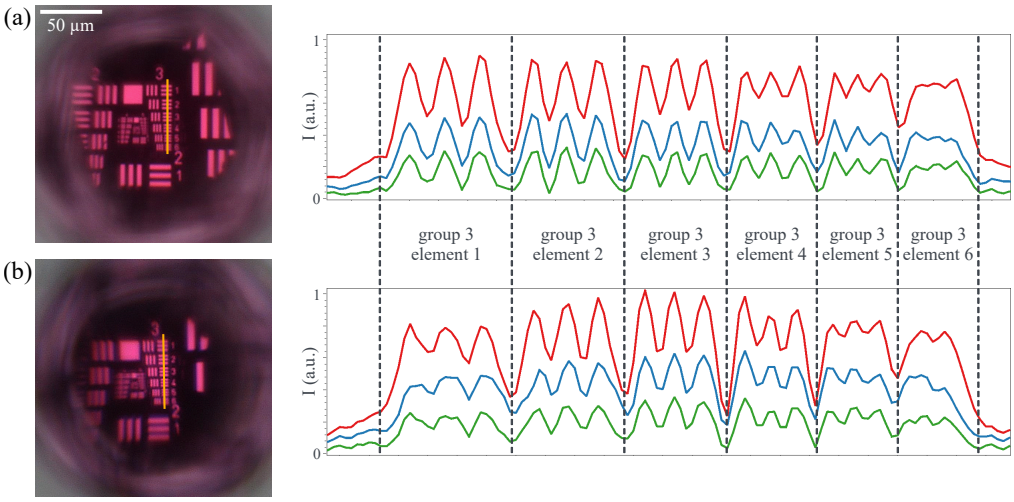

Fig. 5. Long-term stability. Image of the USAF resolution chart (a) taken directly after printing the red SX AR-N lens, and (b) image taken from the same lens three months later, after it was stored under room conditions for that period. For the two recordings the RGB intensity profiles through a cut along the orange lines are shown on the right side.

two recordings, which can also be seen in the RGB intensity profiles, indicating that there is no significant loss of performance of the colored micro-optics over time.

3.5. Color filtering

To demonstrate how the filter effect can be influenced by the thickness of the micro-structures, we exemplarily printed a green 3x3 color-plate matrix with different thicknesses (5 µm, 10 µm, 25 µm, 50 µm, 75 µm, 100 µm, 150 µm, 200 µm, and 250 µm) on a glass substrate. For printing the filter plates, green SX AR-N was added to the IP-S (mixing ratio 1:5) using dyeing method 3. The results are shown in Fig. 6. It is evident that the color impression differs for the different thicknesses. The thin structures are mostly transparent, while the thicker structures have a more saturated green color.

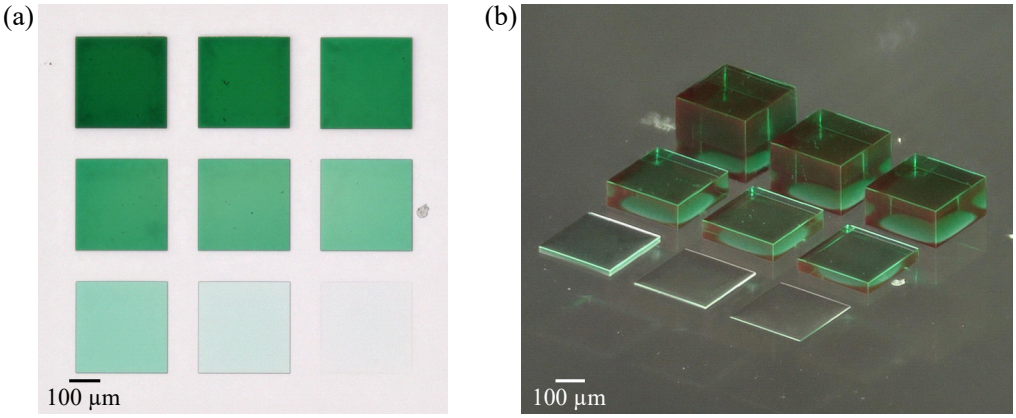

Fig. 6. Microscope images of filter plates. (a) Top view and (b) tilted view of the color-plate matrix, images taken with a digital microscope. The plate thicknesses from top left to bottom right are 250 µm, 200 µm, 150 µm, 100 µm, 75 µm, 50 µm, 25 µm, 10 µm, and 5 µm.

Optical Materials EXPRESS

For a better characterization, we analyzed the light transmitted through the printed plates and through the glass substrate with a spectrometer using the experimental setup shown in Fig. 7. For illumination, a stabilized fiber-coupled light source (wavelength range 360-2600 nm) was used, whose output facet was imaged onto the relevant structures with a 50x microscope objective. This ensures that only the region of interest is illuminated by the light source. In order to gain spectral information, the light that is transmitted through the respective plate is collected with a 20x microscope objective, directed to the spectrometer, and thus recorded. The measurement results are presented in Fig. 8. As the plates were printed on a glass substrate, we took a measurement through the glass substrate only to have a reference spectrum for comparison. The black line marks the reference spectrum, whereas the green lines in Fig. 8(a) show the transmission spectra of the plates of the different thicknesses. Figure 8(b) shows the measured spectra from (a) normalized to the reference spectrum. The intensity of the transmitted light can be modulated by the thickness of the colored structures. The percentage of the intensity of the transmitted light decreases with increasing plate thickness. If one wants a light attenuation, this can be achieved by using thicker elements, which lengthens the optical path of the light through the colored structure and, therefore, increases the proportion of the absorbance. It can be seen that the green filter plates show absorbance especially in the wavelength range from 570 nm to 680 nm, while the transmission for the wavelength range from 450 nm to 570 nm is significantly higher. This shows that the colored resist can be used to attenuate and filter out certain wavelength ranges. The Lambert-Beer law [44] relates the light attenuation to the properties of the used material. We investigated whether the colored filter plates obey the Lambert-Beer law and found a slight deviation in the range of about 1-10% with the largest deviations in the wavelength range around 625 nm. This could be due to the fact that the measured intensities in this range already drop to almost 0 from the filter plate with a thickness of 150 µm. Further information can be found in the supplemental document.

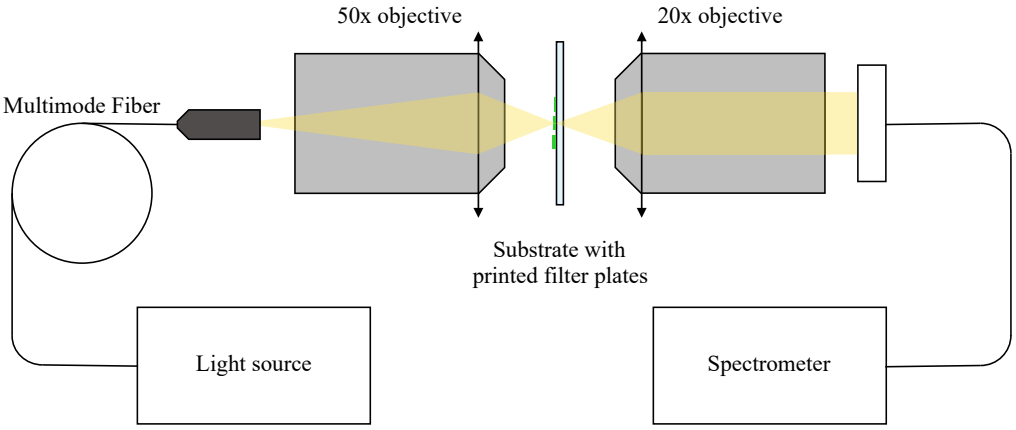

Fig. 7. Experimental setup. The fiber facet of a fiber-coupled white light source is imaged onto the filter plates of the color-plate matrix printed on a glass substrate using a 50x objective. The light that is transmitted through the respective filter plate is then collected with a 20x microscope objective and directed to a spectrometer.

By varying the thickness of the structures and the mixing ratio between the components customized filtering effects can be realized. Also a combination of the different dyes is conceivable. One could, for example, mix multiple dyes of different color into the IP-S or filter stacks consisting of multiple plates of different color could be printed on top of each other. For colored micro-optics, the thicknesses of the lenses could directly be controlled in the optical design to achieve the desired intensity modulation and spectral filtering. Colored structures could also be printed

Optical Materials EXPRESS

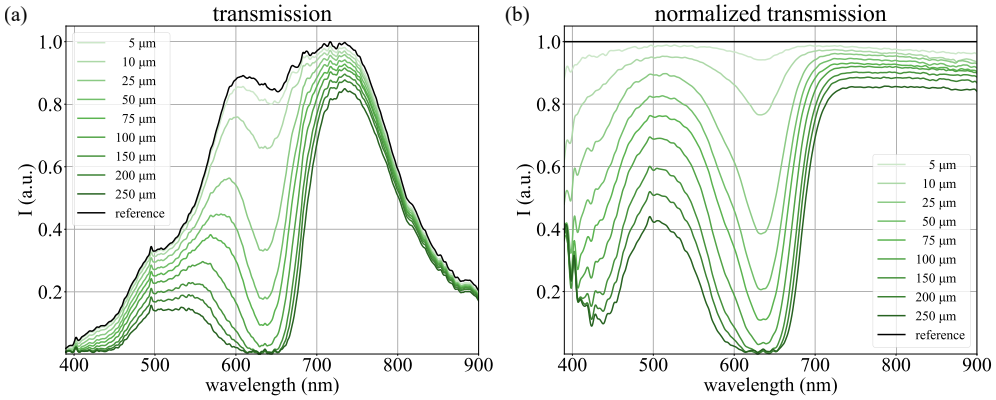

Fig. 8. Transmission Spectra. (a) Transmission spectra through the green plates printed on a glass substrate with different thicknesses from 5 µm to 250 µm and through the glass substrate only as reference. (b) Transmission spectra from (a) normalized to the reference measurement through the glass substrate only. With increasing plate thickness the intensity of the overall transmitted light decreases, while for the green plates the transmission for the wavelength range from 450 nm to 570 nm is still much higher than for the wavelength range from 570 nm to 680 nm.

directly on a sensor to modulate the intensity, shade specific areas and to modify the spectral information of the acquired data. In the field of computer generated holograms, zero order diffraction is a well-known issue. This problem could be addressed by attenuating a specific area of the sensor by printing a small filter plate onto this area. For hyperspectral imaging, multiple micro-optics of different color have to be printed onto a sensor to collect images of the same spatial area at different wavelengths. We took a step towards the field of hyperspectral imaging by printing several micro-optics of different colors using dyeing method 3 (transparent using IP-S only, red using IP-S and red SX AR-N, and yellow using IP-S and yellow SX AR-N) successively on the same glass substrate. The results are shown in Fig. 1(b).

4. Conclusion

We demonstrated three methods for the fabrication of colored micro-structures and micro-optics for spectral filtering and examined their suitability to be used in combination with fs DLW. For the first method the micro-structures were colored in a post-printing process using acetone and the color pigment Eosin Y. For the second method we directly added the Eosin Y to the commonly used photoresist IP-S before printing, and for the third method a colored resist based on an organic dye (SX AR-N) was added to the photopolymer IP-S before the polymerization process. We found that for all three methods the micro-elements could be dyed. However, the first method shows some issues regarding the shape accuracy, and for the second method bubbles occur during the polymerization process resulting in a loss of imaging performance for micro-optical systems.

For the third method, colored micro-optics could be fabricated without a significant imaging performance loss compared to a micro-optical system fabricated using pure IP-S. When examining the long-term stability of the lens systems, also no significant loss in the imaging performance of the colored micro-optics could be found. We measured the refractive index dispersion for the available SX AR-N colors red, yellow, green and blue that where added to IP-S and compared it to a measurement of pure IP-S finding a slightly increased refractive index for the colored resists. Besides the fabrication of colored micro-optical systems, we also showed the fabrication of colored plates, which could be used as filter plates and exemplarily measured the transmission

Optical Materials EXPRESS

spectra for a green color-plate matrix, consisting of plates with different thicknesses from 5 µm to 250 µm. With increasing plate thickness the intensity of the overall transmitted light decreased, while for the green plates the transmission for the wavelength range from 450 nm to 570 nm is still much higher than for wavelengths above this range. Customized filtering effects could be realized by varying the mixing ratio of the components and the thickness of the structures. Here, we focused on the fabrication of colored structures, nevertheless also a black SX AR-N resist is available, to which the manufacturing principle could be transferred to produce micro-elements, especially useful for absorption tasks. In the future, as seen in [32], it could also be tested whether the black ink is suitable for manufacturing different apertures, which could help to reduce stray light. Like for the IP-S, the SX AR-N resists could also be mixed into other commonly used photopolymers using the principle of dyeing method 3.

Our results show successful fs DLW fabrication of colored micro-structures and micro-optics with optical surface quality. The presented dyeing method 3 expands the application area of 3D-printed micro-optics and creates new optical design possibilities, for example towards hyperspectral imaging.

Funding. Deutsche Forschungsgemeinschaft (GRK2543/1); Vector Stiftung (MINT Innovationen); Ministerium für Wissenschaft, Forschung und Kunst Baden-Württemberg (RiSC); Baden-Württemberg Stiftung (Elite Programme for Postdocs); European Research Council (PoC 3D PRINTEDOPTICS); Gips-Schüle-Stiftung (Gips-Schüle Research Award).

Acknowledgments. The work described in this paper was conducted in the framework of the Graduate School 2543/1 "Intraoperative Multi-Sensory Tissue-Differentiation in Oncology" (project A1) funded by the German Research Foundation (DFG - Deutsche Forschungsgemeinschaft). We thank Dr. Maik Gerngross (Allresist GmbH, Strausberg, Germany) for providing us with samples of the SX AR-N resists.

Disclosures. The authors declare no conflicts of interest.

Data availability. Data underlying the results presented in this paper are not publicly available at this time but may be obtained from the authors upon reasonable request.

Supplemental document. See Supplement 1 for supporting content.

References

1. M. Malinauskas, M. Farsari, A. Piskarskas, and S. Juodkazis, "Ultrafast laser nanostructuring of photopolymers: A decade of advances," Phys. Rep. **533**(1), 1–31 (2013).
2. Guo Rui, Xiao Shizhou, Zhai Xiaomin, Li Jiawen, Xia Andong, and Huang Wenhao, "Micro lens fabrication by means of femtosecond two photon photopolymerization," Opt. Express **14**(2), 810–816 (2006).
3. M. Malinauskas, A. Žukauskas, V. Purlys, K. Belazaras, A. Momot, D. Paipulas, R. Gadonas, A. Piskarskas, H. Gilbergs, A. Gaidukevičiutė, I. Sakellari, M. Farsari, and S. Juodkazis, "Femtosecond laser polymerization of hybrid/integrated micro-optical elements and their characterization," J. Opt. **12**(12), 124010 (2010).
4. M. Thiel and M. Hermatschweiler, "Three-dimensional laser lithography," Optik & Photonik **6**(4), 36–39 (2011).
5. K. Sugioka and Y. Cheng, "Femtosecond laser three-dimensional micro- and nanofabrication," Appl. Phys. Rev. **1**(4), 041303 (2014).
6. M. Deubel, G. von Freymann, M. Wegener, S. Pereira, K. Busch, and C. M. Soukoulis, "Direct laser writing of three-dimensional photonic-crystal templates for telecommunications," Nat. Mater. **3**(7), 444–447 (2004).
7. J. K. Hohmann, M. Renner, E. H. Waller, and G. von Freymann, "Three-dimensional µm-printing: An enabling technology," Adv. Opt. Mater. **3**(11), 1488–1507 (2015).
8. M. Malinauskas, A. Žukauskas, S. Hasegawa, Y. Hayasaki, V. Mizeikis, R. Buividas, and S. Juodkazis, "Ultrafast laser processing of materials: from science to industry," Light: Sci. Appl. **5**(8), e16133 (2016).
9. S. Fischbach, A. Schlehahn, A. Thoma, N. Srocka, T. Gissibl, S. Ristok, S. Thiele, A. Kaganskiy, A. Strittmatter, T. Heindel, S. Rodt, A. Herkommer, H. Giessen, and S. Reitzenstein, "Single quantum dot with microlens and 3D-printed micro-objective as integrated bright single-photon source," ACS Photonics **4**(6), 1327–1332 (2017).
10. G. von Freymann, A. Ledermann, M. Thiel, I. Staude, S. Essig, K. Busch, and M. Wegener, "Three-dimensional nanostructures for photonics," Adv. Funct. Mater. **20**(7), 1038–1052 (2010).
11. J. Serbin, A. Egbert, A. Ostendorf, B. N. Chichkov, R. Houbertz, G. Domann, J. Schulz, C. Cronauer, L. Fröhlich, and M. Popall, "Femtosecond laser-induced two-photon polymerization of inorganic-organic hybrid materials for applications in photonics," Opt. Lett. **28**(5), 301–303 (2003).
12. F. Burmeister, S. Steenhusen, R. Houbertz, U. D. Zeitner, S. Nolte, and A. Tünnermann, "Materials and technologies for fabrication of three-dimensional microstructures with sub-100 nm feature sizes by two-photon polymerization," J. Laser Appl. **24**(4), 042014 (2012).

Optical Materials EXPRESS

13. C. Liberale, G. Cojoc, P. Candeloro, G. Das, F. Gentile, F. de Angelis, and E. Di Fabrizio, "Micro-optics fabrication on top of optical fibers using two-photon lithography," IEEE Photonics Technol. Lett. **22**(7), 474–476 (2010).
14. T. Gissibl, S. Thiele, A. Herkommer, and H. Giessen, "Sub-micrometre accurate free-form optics by three-dimensional printing on single-mode fibres," Nat. Commun. **7**(1), 11763 (2016).
15. T. Gissibl, S. Thiele, A. Herkommer, and H. Giessen, "Two-photon direct laser writing of ultracompact multi-lens objectives," Nat. Photonics **10**(8), 554–560 (2016).
16. S. Bianchi, V. P. Rajamanickam, L. Ferrara, E. Di Fabrizio, C. Liberale, and R. Di Leonardo, "Focusing and imaging with increased numerical apertures through multimode fibers with micro-fabricated optics," Opt. Lett. **38**(23), 4935–4938 (2013).
17. S. Thiele, K. Arzenbacher, T. Gissibl, H. Giessen, and A. M. Herkommer, "3D-printed eagle eye: Compound microlens system for foveated imaging," Sci. Adv. **3**(2), e1602655 (2017).
18. A. Toulouse, J. Drozella, P. Motzfeld, N. Fahrbach, V. Aslani, S. Thiele, H. Giessen, and A. M. Herkommer, "Ultra-compact 3D-printed wide-angle cameras realized by multi-aperture freeform optical design," Opt. Express **30**(2), 707–720 (2022).
19. J. Li, S. Thiele, B. C. Quirk, R. W. Kirk, J. W. Verjans, E. Akers, C. A. Bursill, S. J. Nicholls, A. M. Herkommer, H. Giessen, and R. A. McLaughlin, "Ultrathin monolithic 3D printed optical coherence tomography endoscopy for preclinical and clinical use," Light: Sci. Appl. **9**(1), 124 (2020).
20. J. Li, S. Thiele, R. W. Kirk, B. C. Quirk, A. Hoogendoorn, Y. C. Chen, K. Peter, S. J. Nicholls, J. W. Verjans, P. J. Psaltis, C. Bursill, A. M. Herkommer, H. Giessen, and R. A. McLaughlin, "3D-printed micro lens-in-lens for in vivo multimodal microendoscopy," Small **18**(17), 2107032 (2022).
21. H. Eto, H. G. Franquelim, M. Heymann, and P. Schwille, "Membrane-coated 3D architectures for bottom-up synthetic biology," Soft Matter **17**(22), 5456–5466 (2021).
22. A. Selimis, V. Mironov, and M. Farsari, "Direct laser writing: Principles and materials for scaffold 3D printing," Microelectron. Eng. **132**, 83–89 (2015).
23. V. Melissinaki, A. A. Gill, I. Ortega, M. Vamvakaki, A. Ranella, J. W. Haycock, C. Fotakis, M. Farsari, and F. Claeyssens, "Direct laser writing of 3D scaffolds for neural tissue engineering applications," Biofabrication **3**(4), 045005 (2011).
24. J. Knoška, L. Adriano, S. Awel, K. R. Beyerlein, O. Yefanov, D. Oberthuer, G. E. Pe na Murillo, N. Roth, I. Sarrou, P. Villanueva-Perez, M. O. Wiedorn, F. Wilde, S. Bajt, H. N. Chapman, and M. Heymann, "Ultracompact 3D microfluidics for time-resolved structural biology," Nat. Commun. **11**(1), 1–12 (2020).
25. Liao Yang, Cheng Ya, Liu Changning, Song Jiangxin, He Fei, Shen Yinglong, Chen Danping, Xu Zhizhan, Fan Zhichao, Wei Xunbin, Sugioka Koji, and Midorikawa Katsumi, "Direct laser writing of sub-50 nm nanofluidic channels buried in glass for three-dimensional micro-nanofluidic integration," Lab Chip **13**(8), 1626–1631 (2013).
26. A. Toulouse, J. Drozella, S. Thiele, H. Giessen, and A. Herkommer, "3D-printed miniature spectrometer for the visible range with a 100x100 μm^2 footprint," Light: Adv. Manuf. **2**(1), 20–30 (2021).
27. F. Wang, Y. Chong, F. Wang, and C. He, "Photopolymer resins for luminescent three-dimensional printing," J. Appl. Polym. Sci. **134**(32), 44988 (2017).
28. A. P. Haring, A. U. Khan, G. Liu, and B. N. Johnson, "3D printed functionally graded plasmonic constructs," Adv. Opt. Mater. **5**(18), 1700367 (2017).
29. Y. L. Kong, I. A. Tamargo, H. Kim, B. N. Johnson, M. K. Gupta, T.-W. Koh, H.-A. Chin, D. A. Steingart, B. P. Rand, and M. C. McAlpine, "3D printed quantum dot light-emitting diodes," Nano Lett. **14**(12), 7017–7023 (2014).
30. A. Toulouse, S. Thiele, H. Giessen, and A. M. Herkommer, "Alignment-free integration of apertures and nontransparent hulls into 3D-printed micro-optics," Opt. Lett. **43**(21), 5283–5286 (2018).
31. K. Weber, Z. Wang, S. Thiele, A. Herkommer, and H. Giessen, "Distortion-free multi-element hypergon wide-angle micro-objective obtained by femtosecond 3D printing," Opt. Lett. **45**(10), 2784–2787 (2020).
32. M. D. Schmid, A. Toulouse, S. Thiele, S. Mangold, A. M. Herkommer, and H. Giessen, "3D direct laser writing of highly absorptive photoresist for miniature optical apertures," Adv. Funct. Mater. **1**, 2211159 (2022).
33. G. Lu and B. Fei, "Medical hyperspectral imaging: a review," J. Biomed. Opt. **19**(1), 010901 (2014).
34. G. Lu, L. Halig, D. Wang, X. Qin, Z. G. Chen, and B. Fei, "Spectral-spatial classification for noninvasive cancer detection using hyperspectral imaging," J. Biomed. Opt. **19**(10), 106004 (2014).
35. K. Gono, "Narrow band imaging: Technology basis and research and development history," Clin. Endoscopy **48**(6), 476–480 (2015).
36. G. M. Kamphuis, D. M. de Bruin, J Fallert, M. H. Gultekin, T. M. de Reijke, Pes M. P. Laguna, and J. J. M. C. H de la Rosette, "Storz professional image enhancement system: a new technique to improve endoscopic bladder imaging," *Journal of Cancer Science & Therapy* (2016).
37. K. Kuznetsov, R. Lambert, and J.-F. Rey, "Narrow-band imaging: potential and limitations," Endoscopy **38**(01), 76–81 (2006).
38. E. C. Cauberg, S. Kloen, Visser M. de la Rosette, J. M. C. H. Jean, M. Babjuk, V. Soukup, M. Pesl, J. Duskova, and T. M. de Reijke, "Narrow band imaging cystoscopy improves the detection of non–muscle-invasive bladder cancer," Urology **76**(3), 658–663 (2010).
39. H. W. Herr and S. M. Donat, "A comparison of white-light cystoscopy and narrow-band imaging cystoscopy to detect bladder tumour recurrences," BJU Int. **102**(9), 1111–1114 (2008).

Optical Materials EXPRESS

40. A. Toulouse, S. Thiele, K. Hirzel, M. Schmid, K. Weber, M. Zyrianova, H. Giessen, A. M. Herkommer, and M. Heymann, "High resolution femtosecond direct laser writing with wrapped lens," Opt. Mater. Express **12**(9), 3801 (2022).
41. NanoGuide, "Adding Color to IP-Q Structures (Dyeing)," (https://support.nanoscribe.com/hc/en-gb/articles/360009627139-Adding-Color-to-IP-Q-Structures-Dyeing-, 08.03.2023).
42. Allresist GmbH, "Eingefärbte Negativ-Photoresists," (https://www.allresist.de/eingefaerbte-negativ-photoresists/, 08.03.2023).
43. M. Schmid, D. Ludescher, and H. Giessen, "Optical properties of photoresists for femtosecond 3D printing: refractive index, extinction, luminescence-dose dependence, aging, heat treatment and comparison between 1-photon and 2-photon exposure," Opt. Mater. Express **9**(12), 4564 (2019).
44. D. F. Swinehart, "The Beer-Lambert law," J. Chem. Educ. **39**(7), 333 (1962).